Error of an arbitrary single-mode Gaussian transformation on a weighted cluster state using a cubic phase gate

E. R. Zinatullin,[1] S. B. Korolev,[1] A. D. Manukhova,[2] and T. Yu. Golubeva[1]
[1]*Department of Physics, St. Petersburg State University, Universitetskaya Náberezhnaya 7/9, St. Petersburg 199034, Russia*
[2]*Department of Optics, Palacký University, 17 Listopadu 12, Olomouc 771 46, Czech Republic*

(Received 4 July 2022; accepted 26 August 2022; published 12 September 2022)

In this paper we propose two strategies for decreasing the error of arbitrary single-mode Gaussian transformations implemented using one-way quantum computation on a four-node linear cluster state. We show that it is possible to minimize the error of the arbitrary single-mode Gaussian transformation by a proper choice of the weight coefficients of the cluster state. We modify the computation scheme by adding a non-Gaussian state obtained using a cubic phase gate as one of the nodes of the cluster. This further decreases the computation error. We evaluate the efficiencies of the proposed optimization schemes comparing the probabilities of the error correction of the quantum computations with and without optimizations. We show that for some transformations, the error probability can be reduced by up to 900 times.

DOI: 10.1103/PhysRevA.106.032414

I. INTRODUCTION

The main goal of quantum information and quantum computation is so-called universal quantum computation. This universal quantum computation can effect any unitary transformation over a finite number of variables to any degree of precision [1] using the repeated application of local operations (affecting only a few variables at the same time). One-way quantum computation [2–4] is a promising model for universal quantum computation. In our work we discuss the continuous-variable one-way quantum computation technique [2]. Unlike discrete quantum systems, the use of continuous variables allows one to build schemes that give a significant measurement result each time they are addressed (deterministic circuits). Moreover, such systems have great potential in terms of their scalability [5–10]. To achieve the universality of quantum computation, with continuous variables, it is necessary to be able to implement an arbitrary single-mode Gaussian (linear) transformation, a two-mode transformation, and at least one non-Gaussian (nonlinear) transformation [1].

The main resources of one-way quantum computation are cluster states. These states belong to the family of highly entangled multipartite quantum states. Such states can be effectively parametrized by a mathematical graph [11]. There are many ways to implement cluster states in continuous variables. It can be implemented with optomechanical systems [12], atomic ensembles [13], hybrid variables [14], mixed (atomic-field) systems [15,16], and light fields [17–21].

In continuous variables, cluster states are generated via a set of squeezed oscillators. In the idealized case, when the fluctuations in the squeezed quadrature are completely suppressed, the operations in the considered model are performed without errors. However, in reality, it is impossible to obtain an ideal squeezed state; oscillators with finite squeezing are used to generate a cluster. As a result, noises from nonideal squeezed quadratures distort the result of operations and lead to the appearance of inherent errors. The presence of these errors is the main limiting factor for the model under consideration. At the moment, the experimentally feasible squeezing is insufficient for performing fault-tolerant universal one-way quantum computations. The maximum achieved is -15 dB [22], whereas the minimum required value for such computations (without using surface codes and the postselection procedure) is -20.5 dB [23].

There are various methods to get around the limitations associated with insufficient squeezing. Such methods include the use of postselection [24] and surface codes [24–30]. For example, in [24] the authors proposed a computation scheme that makes it possible to reduce the squeezing requirements to -10.8 dB. However, the main efforts are usually directed at error correction, while we propose to modify the computation scheme itself. The resource state requirement can be lowered by using computation schemes less sensitive to the inherent error. The idea of constructing such schemes is to analyze the computational procedure to identify the nodes giving the noisiest result and reduce their influence. Reducing errors in just one of the classes of operations necessary for universal quantum computation helps to reduce the requirements for the resource state for the entire scheme.

The main goal of our work is to reduce arbitrary single-mode Gaussian operation errors. The first strategy is to employ the Gaussian transformations and to vary the weight coefficients of the cluster state used as a resource for the quantum computation. In [31], based on the quantum teleportation protocol, we showed that it is possible to decrease the quantum signal transmission error by using the weighted controlled-Z (CZ) transformation [32–34] as an entanglement operation. Increasing the weight coefficients made it possible to significantly decrease the error in one of the quadratures while the transformation remains Gaussian. Therefore, in

Sec. II we study the impact of the cluster state weight coefficients on the single-mode operation errors.

It is necessary to mention that, according to the no-go theorem [35], Gaussian states cannot be used to correct Gaussian errors (determined by Gaussian transformations) in Gaussian states. The proposed method does not contradict this theorem. We reduce the computation error not by additional error correction, but by reducing the impact of the nodes that contribute the most errors.

The second strategy for decreasing the error is to use the clusters with non-Gaussian nodes. In [36] we showed that it is possible to reduce the errors in the teleportation protocol by using the states prepared with the cubic phase gate [37]. The teleportation protocol underlies the one-way quantum computation. Therefore, we apply the strategy of cluster modification to perform computation with fewer errors. At the same time, we place the emphasis on the minimum change in the resource state (modifying only one node), which would lead to a decrease of the maximum error. It is worth noting that the chosen non-Gaussian operation can be performed deterministically, when each measurement leads to the desired result. This is important for the scalability of quantum computation schemes and is advantageous for computations with continuous variables. Probabilistic procedures (such as photon subtraction [38,39]) would deprive the protocol of this advantage.

In [36] we proposed a strategy for decreasing the quantum teleportation protocol error by using a cubic phase gate to prepare a non-Gaussian resource state. In Sec. III we apply this strategy to decrease the error of arbitrary single-mode Gaussian transformations. We note that the generation of cubic phase states is also a challenging experimental problem. The first idea of cubic phase state generation was proposed by Gottesman *et al.* [37,40,41]. It turned out that this idea is difficult to implement. It requires performing the quadrature displacement operation by a value far from what is achievable in an experiment. The cubic phase gate has long been an abstract mathematical transformation not realizable. This situation has changed in recent years. Many works have been devoted to methods for cubic phase state generation [42–44] and the implementation of the cubic phase gate [45–49] phenomena. Particularly significant progress was achieved in the microwave frequency range; it was in this range that the cubic phase state was generated for the first time [50]. As a result, the cubic phase gate gradually turns from a purely theoretical transformation into a real-life device.

The paper is organized as follows. In Sec. II we describe the transformation scheme on a weighted four-node linear cluster state and demonstrate its arbitrariness for any values of weight coefficients. Also in this section we estimate the errors in the scheme considered and options proposed for optimizing the transformation errors for experimentally achievable values of the weight coefficients. In Sec. III we study a modified computation scheme in which a cubic phase gate is used to prepare the cluster state, estimate the errors in this scheme, and perform their optimization. In Sec. IV we evaluate the efficiency of optimization of the computation proposed in the previous sections based on the calculation of the error correction probability.

II. ARBITRARY SINGLE-MODE GAUSSIAN OPERATION ON A FOUR-NODE CLUSTER

A. Transformation scheme on a linear four-node weighted cluster

The principle of performing an arbitrary single-mode Gaussian operation on an unweighted linear four-node cluster is well known [41,51]. In this section we repeat similar transformations on a weighted cluster and in the next section we will demonstrate their arbitrariness for any values of the weight coefficients.

To get an explicit expression for the transformation error, let us start with constructing the cluster state. The linear cluster state [Fig. 1(a)] is prepared from four oscillators squeezed in the y quadrature. The quadratures of the jth oscillator are described as

$$\hat{x}_{s,j} = e^{r}\hat{x}_{0,j}, \quad \hat{y}_{s,j} = e^{-r}\hat{y}_{0,j}, \tag{1}$$

where r is the squeezing coefficient and $\hat{x}_{0,j}$ and $\hat{y}_{0,j}$ are the quadratures of the jth oscillator in the vacuum state. The entanglement of cluster nodes with each other, as well as the entanglement of an input state with the node of the cluster state, will be carried out by using the CZ gate with the weight coefficients g_{jk}. This transformation acts on the oscillators j and k as

$$\hat{C}_z(g_{jk}) = e^{2ig_{jk}\hat{x}_j\hat{x}_k}. \tag{2}$$

The weight coefficient g_{jk} of the CZ gate can take any real value. The value of the weight coefficient determines the strength of the entanglement, i.e., how much information about the jth system after the entanglement procedure will be contained in the kth and vice versa. The sign of the weight coefficient indicates the creation of positive or negative correlations (anticorrelations) between oscillators. Hereinafter, in the paper we consider positive weight coefficients, bearing in mind that their sign does not influence the error decrease.

All CZ transformations commute with each other. Thus, we can consider the computation on a four-node cluster state [see Fig. 1(b)] as a computation on a pair of two-node cluster states [see Fig. 1(c)]. It simplifies the analysis of the scheme.

Let us consider the transformation performed on the first pair of resource states. The first and second squeezed oscillators are entangled using the CZ gate with the weight coefficient g_1. The input state is entangled with the first resource oscillator by a similar operation with a weight coefficient g_4. As the result, the amplitudes of the oscillators take the form

$$\hat{a}'_{\text{in}} = \hat{x}_{\text{in}} + i(\hat{y}_{\text{in}} + g_4\hat{x}_{s,1}), \tag{3}$$

$$\hat{a}'_1 = \hat{x}_{s,1} + i(\hat{y}_{s,1} + g_1\hat{x}_{s,2} + g_4\hat{x}_{\text{in}}), \tag{4}$$

$$\hat{a}'_2 = \hat{x}_{s,2} + i(\hat{y}_{s,2} + g_1\hat{x}_{s,1}). \tag{5}$$

We then perform homodyne measurements with the local oscillator's phases θ_1 and θ_2 over the input and first oscillators, respectively. It leads to the equalities for the photocurrent

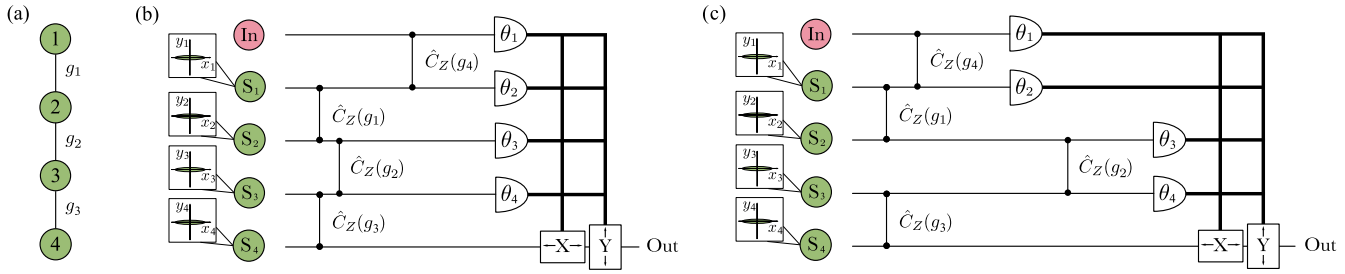

FIG. 1. (a) Configuration of the cluster state used as a resource for computation. (b) Scheme for implementing the arbitrary single-mode Gaussian operation on a linear weighted four-node cluster state. (c) Scheme of implementation of arbitrary single-mode Gaussian operation on a pair of two-node cluster states. In the diagram, In is the input state, S_j are squeezed states, $\hat{C}_z(g_j)$ is the CZ transformation with weight coefficient g_j, θ_j are the phases of the local oscillators employed for a balanced homodyne detection, and X and Y are operations that displace the corresponding quadratures of the fields in the channel, depending on the detection results.

operators

$$\hat{i}_{\rm in} = \beta \sin\theta_1(\hat{y}_{\rm in} + g_4\hat{x}_{s,1}) + \beta\cos\theta_1\hat{x}_{\rm in}, \tag{6}$$

$$\hat{i}_1 = \beta \sin\theta_2(\hat{y}_{s,1} + g_1\hat{x}_{s,2} + g_4\hat{x}_{\rm in}) + \beta\cos\theta_2\hat{x}_{s,1}, \tag{7}$$

where β is the amplitude of the homodyne detector's local oscillator. Such measurements, due to the entanglement of the resource state, lead to a change in the quadrature components of the second oscillator:

$$\hat{x}_2' = \left(\frac{\cot\theta_1\cot\theta_2}{g_1g_4} - \frac{g_4}{g_1}\right)\hat{x}_{\rm in} + \frac{\cot\theta_2}{g_1g_4}\hat{y}_{\rm in} - \frac{\hat{y}_{s,1}}{g_1} + \frac{i_{1,m}}{\beta g_1\sin\theta_2} - \frac{i_{{\rm in},m}\cot\theta_2}{\beta g_1g_4\sin\theta_1}, \tag{8}$$

$$\hat{y}_2' = -\frac{g_1\cot\theta_1}{g_4}\hat{x}_{\rm in} - \frac{g_1}{g_4}\hat{y}_{\rm in} + \hat{y}_{s,2} + \frac{i_{{\rm in},m}g_1}{\beta g_4\sin\theta_1}. \tag{9}$$

Here we replaced the operators of photocurrents with c-numbers corresponding to the results of the given measurement: $i_{1,m}$ and $i_{{\rm in},m}$. Let us rewrite this transformation in a matrix form

$$\begin{pmatrix}\hat{x}_2'\\ \hat{y}_2'\end{pmatrix} = \begin{pmatrix}\frac{\cot\theta_1\cot\theta_2}{g_1g_4} - \frac{g_4}{g_1} & \frac{\cot\theta_2}{g_1g_4}\\ -\frac{g_1\cot\theta_1}{g_4} & -\frac{g_1}{g_4}\end{pmatrix}\begin{pmatrix}\hat{x}_{\rm in}\\ \hat{y}_{\rm in}\end{pmatrix} + \begin{pmatrix}-\frac{\hat{y}_{s,1}}{g_1}\\ \hat{y}_{s,2}\end{pmatrix} + \begin{pmatrix}\frac{i_{1,m}}{\beta g_1\sin\theta_2} - \frac{i_{{\rm in},m}\cot\theta_2}{\beta g_1g_2\sin\theta_1}\\ \frac{i_{{\rm in},m}g_1}{\beta g_2\sin\theta_1}\end{pmatrix}. \tag{10}$$

It is well known that this Gaussian transformation is not arbitrary for the unit weight coefficients. To ensure arbitrariness, it is necessary to perform a similar operation again on another pair of nodes. Since our goal is to ensure arbitrariness for any g_j, and for $g_j = 1$ it is not arbitrary, the scheme needs to be complemented.

The operation on the second pair of nodes, up to weight coefficients of the CZ gate, repeats the operation on the first pair of nodes. Thus, the second part of the scheme operates similarly to the transformation (10), where the input data are the quadratures x_2' and y_2'. At the output of the scheme, the c-number components of the quadratures of the field are compensated by displacement, depending on the values of the measured photocurrents. We introduce new notation

$$\cot\theta_2' = \frac{\cot\theta_2}{g_4^2}, \quad \cot\theta_4' = \frac{\cot\theta_4}{g_2^2}. \tag{11}$$

Note that in the new notation, the mathematical expression for the input-output transformation will depend not on the weight coefficients themselves, but on their ratio. It is convenient for further analysis. Thus, the operation carried out by our scheme has the form

$$\begin{pmatrix}\hat{x}_{\rm out}\\ \hat{y}_{\rm out}\end{pmatrix} = U(\theta_1,\theta_2',\theta_3,\theta_4')\begin{pmatrix}\hat{x}_{\rm in}\\ \hat{y}_{\rm in}\end{pmatrix} + \delta\hat{\mathbf{e}}_0(\theta_3,\theta_4'). \tag{12}$$

Here the desired transformation performed on the input state is described by the matrix

$$U(\theta_1,\theta_2',\theta_3,\theta_4') = \begin{pmatrix}\frac{\cot\theta_3\cot\theta_4'-1}{g_3/g_2} & \frac{\cot\theta_4'}{g_3/g_2}\\ -\frac{g_3\cot\theta_3}{g_2} & -\frac{g_3}{g_2}\end{pmatrix} \times \begin{pmatrix}\frac{\cot\theta_1\cot\theta_2'-1}{g_1/g_4} & \frac{\cot\theta_2'}{g_1/g_4}\\ -\frac{g_1\cot\theta_1}{g_4} & -\frac{g_1}{g_4}\end{pmatrix} \tag{13}$$

and the transformation error associated with the finite squeezing of the oscillators is described by the vector

$$\delta\hat{\mathbf{e}}_0(\theta_3,\theta_4') = \begin{pmatrix}\frac{\cot\theta_3\cot\theta_4'-1}{g_3/g_2} & \frac{\cot\theta_4'}{g_3/g_2}\\ -\frac{g_3\cot\theta_3}{g_2} & -\frac{g_3}{g_2}\end{pmatrix}\begin{pmatrix}-\frac{\hat{y}_{s,1}}{g_1}\\ \hat{y}_{s,2}\end{pmatrix} + \begin{pmatrix}-\frac{\hat{y}_{s,3}}{g_3}\\ \hat{y}_{s,4}\end{pmatrix}. \tag{14}$$

It should be noted that in the scheme under consideration, the transformation error $\delta\hat{\mathbf{e}}_0$ depends only on the angles θ_3 and θ_4'. This is because measuring the second pair of resource oscillators transforms the error from the first pair of resource oscillators.

B. Arbitrariness of the transformation with arbitrary weight coefficients

First, we need to find out if the single-mode Gaussian transformation U is arbitrary. It was shown in [51] that the U will be arbitrary when weight coefficients of the CZ gate are unity. However, we need to check whether arbitrariness is preserved for arbitrary nonunity weight coefficients. To do this, we will show that it is possible to choose the phases of local oscillators of homodyne detectors in such a way that the matrix $U(\theta_1,\theta_2',\theta_3,\theta_4')$ is equal to any given arbitrary symplectic matrix, i.e.,

$$U(\theta_1,\theta_2',\theta_3,\theta_4') = \begin{pmatrix}a & b\\ c & d\end{pmatrix}, \tag{15}$$

where the coefficients of the matrix satisfy the condition

$$ad - bc = 1. \tag{16}$$

Taking into account the explicit form (13) of the matrix U, Eq. (15) is equivalent to the system of equations

$$\frac{g_2 g_4}{g_1 g_3}(\cot\theta_1 \cot\theta_2' - 1)(\cot\theta_3 \cot\theta_4' - 1) - \frac{g_1 g_2}{g_3 g_4}\cot\theta_1 \cot\theta_4' = a, \tag{17}$$

$$\frac{g_2 g_4}{g_1 g_3}\cot\theta_2'(\cot\theta_3 \cot\theta_4' - 1) - \frac{g_1 g_2}{g_3 g_4}\cot\theta_4' = b, \tag{18}$$

$$-\frac{g_3 g_4}{g_1 g_2}(\cot\theta_1 \cot\theta_2' - 1)\cot\theta_3 + \frac{g_1 g_3}{g_2 g_4}\cot\theta_1 = c, \tag{19}$$

$$-\frac{g_3 g_4}{g_1 g_2}\cot\theta_2' \cot\theta_3 + \frac{g_1 g_3}{g_2 g_4} = d. \tag{20}$$

Due to the condition (16) on the matrix coefficients, any one of these equations can be derived from the three remaining ones. Thus, there are only three independent equations in four variables. The system of equations (17)–(20) is not uniquely solved and one of the phases can be chosen as a free parameter, which we can change. We can see that for $\theta_2' = \pi/2$ or $\theta_3 = \pi/2$ Eq. (20) turns into equality so that we lose the ability to solve the system for an arbitrary matrix. Therefore, the phases θ_2' and θ_3 cannot be chosen as free parameters. Of the remaining two phases, the phase θ_4' is the best candidate to be a free parameter, since the transformation error depends on it. In the future, with the right choice of the phase θ_4', we will be able to minimize the transformation error.

For some arbitrary fixed value of the phase θ_4', the solution of the system (17)–(20) exists for the remaining phases and has the form

$$\cot\theta_1 = \frac{c}{d} + \frac{\left(\frac{g_1 g_3}{g_2 g_4} - d\right)\frac{g_3}{g_2}}{\left(\frac{g_3^2}{g_2^2}b + d\cot\theta_4'\right)\frac{g_1}{g_4}d}, \tag{21}$$

$$\cot\theta_2' = -\frac{g_1 g_2}{g_3 g_4}\left(\frac{g_3^2}{g_2^2}b + d\cot\theta_4'\right), \tag{22}$$

$$\cot\theta_3 = \frac{d - \frac{g_1 g_3}{g_2 g_4}}{\frac{g_3^2}{g_2^2}b + d\cot\theta_4'}. \tag{23}$$

Thus, for any arbitrary fixed value θ_4', we can choose the phases of the local oscillators θ_1, θ_2', and θ_3 in such a way that the matrix (13) is equal to any given arbitrary symplectic matrix. This means that the single-mode Gaussian transformation given by the matrix (13) is arbitrary.

C. Single-mode transformation error on a weighted cluster

1. Optimization for arbitrary values of weight coefficients

Let us estimate the errors in the scheme of one-way computations considered. To do this, we pass from the error vector to one consisting of variances $\langle\delta\hat{\mathbf{e}}_0^2\rangle$. We assume resource oscillators to be statistically independent and squeezed equally, i.e., $\langle\hat{y}_{s,j}^2\rangle \equiv \langle\delta\hat{y}_s^2\rangle$ for $j \in 1, 2, 3, 4$. Then the vector of variances has the form

$$\langle\delta\hat{\mathbf{e}}_0^2\rangle = \begin{pmatrix} \frac{1}{g_1^2}\left(\frac{\cot\theta_3 \cot\theta_4' - 1}{g_3/g_2}\right)^2 + \left(\frac{\cot\theta_4'}{g_3/g_2}\right)^2 + \frac{1}{g_3^2} \\ \frac{1}{g_1^2}\left(\frac{g_3\cot\theta_3}{g_2}\right)^2 + \frac{g_3^2}{g_2^2} + 1 \end{pmatrix}\langle\delta\hat{y}_s^2\rangle. \tag{24}$$

Note that the transformation errors directly depend on the weight coefficients g_1 and g_3. On the other hand, the ratio between weight coefficients g_3/g_2 determines which type of operation at certain phase values is performed. Therefore, it makes sense to compare the transformation errors only for a fixed ratio g_3/g_2, i.e., to compare the errors of the same operations. To achieve it, let us substitute the solutions (21)–(23) into Eq. (24). As a result, we get the error variance vector

$$\langle\delta\hat{\mathbf{e}}_0^2\rangle = \begin{pmatrix} \frac{1}{g_3^2} + \left(\frac{g_2}{g_3}\right)^2\cot^2\theta_4' + \frac{g_2^2\left(b\frac{g_4}{g_1} + \frac{g_2}{g_3}\cot\theta_4'\right)^2}{g_3^2 g_4^2[b + d\left(\frac{g_2}{g_3}\right)^2\cot\theta_4']^2} \\ 1 + \frac{1}{\left(\frac{g_2}{g_3}\right)^2} + \frac{(d\frac{g_2}{g_3}\frac{g_4}{g_1} - 1)^2}{g_4^2[b + d\left(\frac{g_2}{g_3}\right)^2\cot\theta_4']^2} \end{pmatrix} \times \langle\delta\hat{y}_s^2\rangle. \tag{25}$$

This vector depends on the operation implemented (on the values of d and b), on the phase θ_4', and on the value of the weight coefficients of the cluster state g_1, g_2, g_3, and g_4.

The dependence of the error on the weight coefficients of the cluster state means that for each transformation (for each b and d) there is a cluster state configuration that yields the minimal error. One can use this feature to construct nonuniversal quantum calculators capable of solving specific tasks. Here and below we will be interested in the errors of universal quantum computation. Therefore, we omit from consideration calculators for local problems (which are usually called quantum simulators). Unfortunately, in practice, when building a universal computer, we cannot choose weight coefficients for each transformation, since this would require us to rebuild the cluster generation scheme each time. In reality, we have a cluster state with fixed weight coefficients. We need to choose the weight coefficients so that any transformation has a small error. Our goal is to identify such weight coefficients.

From Eq. (25) we can see that if we impose the conditions on the weight coefficients $g_1 \gg g_4$, $g_2 \gg g_3$, $g_3 \gg 1$, and $g_4 \gg 1$ and set θ_4' equal to $\pi/2$, then the error will be proportional to the vector

$$\langle\delta\hat{\mathbf{e}}_0^2\rangle \approx \begin{pmatrix} 0 \\ 1 \end{pmatrix}\langle\delta\hat{y}_s^2\rangle, \tag{26}$$

that is, we get the minimum computation error, which does not depend on the implemented operations (on b and d). Unfortunately, in experiments, we cannot make the weight coefficients infinitely large, since that would require infinite squeezed resource states. Let us see how large we can make them in practice.

2. Experimental implementation of the CZ transformation

To understand what restrictions are imposed on the weight coefficients of the cluster state, let us consider the structure of the CZ transformation. As is known, the CZ gate with the weight coefficient g transforms the vector of input quadratures into the vector of output quadratures according to the rule

$$\begin{pmatrix} \hat{X}_{\text{out},1} \\ \hat{X}_{\text{out},2} \\ \hat{Y}_{\text{out},1} \\ \hat{Y}_{\text{out},2} \end{pmatrix} = \begin{pmatrix} 1 & 0 & 0 & 0 \\ 0 & 1 & 0 & 0 \\ 0 & g & 1 & 0 \\ g & 0 & 0 & 1 \end{pmatrix}\begin{pmatrix} \hat{x}_{\text{in},1} \\ \hat{x}_{\text{in},2} \\ \hat{y}_{\text{in},1} \\ \hat{y}_{\text{in},2} \end{pmatrix}. \tag{27}$$

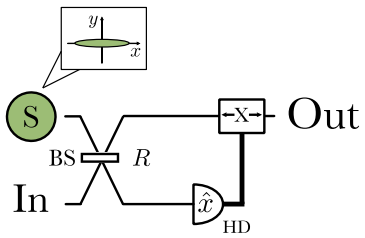

FIG. 2. Implementation of in-line squeezing.

To understand how this transformation can be implemented experimentally, we need to use the Bloch-Messiah decomposition for the CZ matrix, which has the form

$$\begin{pmatrix}1&0&0&0\\0&1&0&0\\0&g&1&0\\g&0&0&1\end{pmatrix}=\begin{pmatrix}1&0&0&0\\0&0&0&-1\\0&0&1&0\\0&1&0&0\end{pmatrix}\begin{pmatrix}t&r&0&0\\r&-t&0&0\\0&0&t&r\\0&0&r&-t\end{pmatrix}\times\begin{pmatrix}\sqrt{s}&0&0&0\\0&\frac{1}{\sqrt{s}}&0&0\\0&0&\frac{1}{\sqrt{s}}&0\\0&0&0&\sqrt{s}\end{pmatrix}\times\begin{pmatrix}r&t&0&0\\t&-r&0&0\\0&0&r&t\\0&0&t&-r\end{pmatrix}\times\begin{pmatrix}1&0&0&0\\0&0&0&1\\0&0&1&0\\0&-1&0&0\end{pmatrix},\tag{28}$$

where

$$r=\frac{\sqrt{s}}{\sqrt{1+s}},\quad t=\frac{1}{\sqrt{1+s}},\qquad s=\frac{1}{2}\left(2+g^2-g\sqrt{4+g^2}\right).\tag{29}$$

Here the first and last matrices describe the phase shifters, the second and fourth matrices describe the beam splitter transformation, and the third matrix describes the squeezing. Since we consider the case of non-negative weight coefficients $g, s \in [0, 1]$.

The main difficulty in the practical implementation of the CZ gate is the in-line squeezing. The in-line squeezing is the squeezing transformation performed on the oscillator inside the computation scheme. For in-line squeezing of the oscillator in one of the quadratures, the scheme shown in Fig. 2 is usually applied. In this scheme, the squeezed state S is entangling with the input state (In) (the state we are transforming) on the beam splitter with a reflection coefficient R. Next the x quadrature of the state in the lower channel is measured using the homodyne detector. After that, the measurement result is sent to a device that displaces the quadratures of the state in the upper channel (the device is indicated by X in the diagram) depending on the measurement result. The quadratures of the output state (Out) can be represented as

$$\begin{pmatrix}\hat{X}_{\rm out}\\ \hat{Y}_{\rm out}\end{pmatrix}=\begin{pmatrix}\frac{1}{\sqrt{R}}&0\\0&\sqrt{R}\end{pmatrix}\begin{pmatrix}\hat{x}_{\rm in}\\ \hat{y}_{\rm in}\end{pmatrix}+\begin{pmatrix}0\\ \sqrt{1-R}\hat{y}_s\end{pmatrix}.\tag{30}$$

It can be seen from this expression that the quadrature $\sqrt{R}\hat{y}_{\rm in}$ is squeezed, since the reflection coefficient is in the range $R \in [0, 1]$. Since the squeezing coefficient s in Eq. (29) is in the range $s \in [0, 1]$, we can set $s = R$, implying that the reflection coefficient is responsible for the squeezing. As we can see, the main bottleneck of this implementation of the squeezing transformation is that there is an error that is added to the computation results. This error is proportional to the squeezed quadrature of the auxiliary oscillator S. The more the quadrature is squeezed, the better the gate is realized.

We use the considered scheme as part of the CZ transformation. Let us estimate the squeezing of the auxiliary quantum oscillators required for this. For the error to remain small compared to the main transformation, the requirement

$$(1-R)\langle\delta\hat{y}_s^2\rangle \ll R\langle\delta\hat{y}_{\rm in}^2\rangle\tag{31}$$

must be met or

$$10\log_{10}\left[4\langle\delta\hat{y}_s^2\rangle\right] \ll 10\log_{10}\left[\frac{4R}{1-R}\langle\delta\hat{y}_{\rm in}^2\rangle\right].\tag{32}$$

In this section, for simplicity, we consider fluctuations of the coherent state ($\langle\delta\hat{y}_{\rm in}^2\rangle = \frac{1}{4}$) as a variance of the input state.

To understand what kind of squeezing we can implement experimentally, we write the expression in a general form for an arbitrary g. To do this, we take into account the equality $s = R$ and substitute the relationship (29) between the values of the squeezing ratio s and the weight coefficient g into Eq. (32). As a result, the final dependence of the weight coefficient on the squeezing of the auxiliary oscillator can be estimated by the inequality

$$g < \frac{10^{-x/20}}{\sqrt{1+10^{x/10}}},\tag{33}$$

where $x = 10\log_{10}(4\langle\delta\hat{y}_s^2\rangle)$. For greater clarity, Eq. (33) is shown in Fig. 3. At the moment, the squeezing that has been experimentally demonstrated is -15 dB [22]. Given the fact that the error should be small compared to the main transformation, we can say that the weight coefficient g can be no more than 5. We use this value further for numerical estimates, as corresponding to the maximum experimentally realized squeezing.

3. Optimization of errors of one-way transformations for bounded values of g

Let us compare the computation errors with different weight coefficients. We consider the $\|\cdot\|_\infty$-norm as a measure of errors. This norm has the form $\|\langle\delta\hat{\mathbf{e}}_0^2\rangle\|_\infty = \max[\langle\delta\hat{\mathbf{e}}_0^2\rangle_1, \langle\delta\hat{\mathbf{e}}_0^2\rangle_2]$.

As we have discussed, to minimize the error, we require the conditions $g_1 \gg g_4$, $g_2 \gg g_3$, $g_3 \gg 1$, $g_4 \gg 1$, and $\theta_4' = \pi/2$. From the first two inequalities, we can conclude that g_1 and

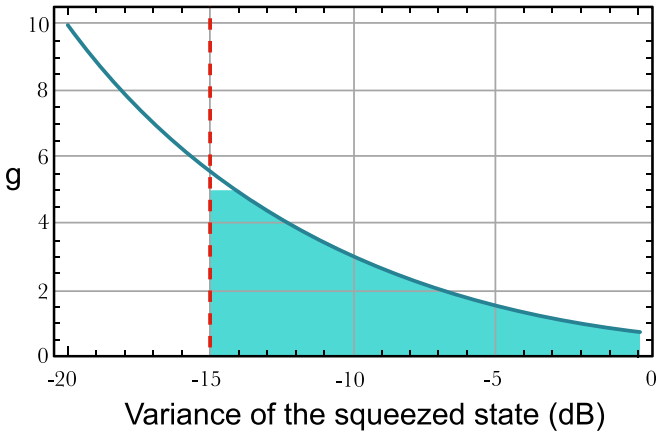

FIG. 3. Graph of the dependence of the value of the CZ gate weight coefficient on the variance of the squeezed oscillator used to implement this transformation. On the graph, the blue solid line indicates the dependence of the weight coefficient on the variance of the squeezed state and the red dotted line indicates the squeezing limit experimentally implemented to date.

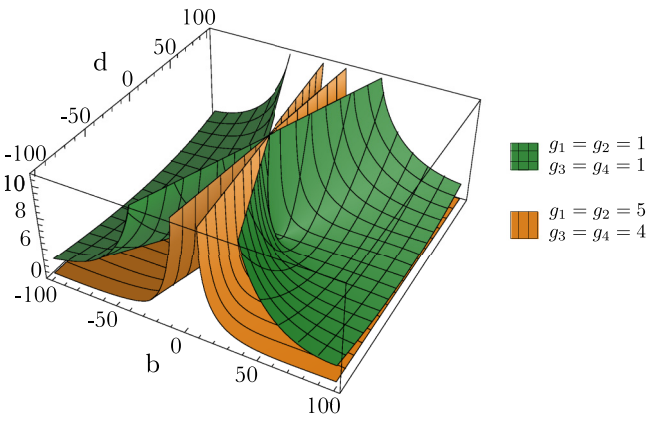

FIG. 4. Distribution of errors $\|\langle\delta\hat{\mathbf{e}}_0^2\rangle\|_\infty/\langle\delta\hat{y}_s^2\rangle$ depending on the implemented single-mode transformation, i.e., depending on b and d [see Eq. (15)]. The graph shows two error surfaces corresponding to computations on two cluster states. The lower surface corresponds to the case of computations on a weighted optimized cluster state ($g_1 = g_2 = 5$ and $g_3 = g_4 = 4$). The upper surface corresponds to the computational errors on the unweighted cluster state ($g_1 = g_2 = g_3 = g_4 = 1$).

g_2 should be chosen as maxima, i.e., $g_1 = g_2 = 5$. It follows from the remaining conditions that g_3 and g_4 should be large enough (compared to unity), so we choose $g_3 = g_4 = 4$. As before, we investigate the effect of weight coefficients on transformation errors for $\theta_4' = \pi/2$.

It should be noted that one can carry out a multidimensional optimization to find the global minimum of computation errors. However, this is a computationally difficult problem. In addition, the global minimum may lie outside the admissible weight coefficients. In this regard, we limit ourselves to the selection of weight coefficients of the cluster state, which provides a smaller error for a larger number of operations.

We first compare the errors for computation on a cluster state with the optimized weight coefficients ($g_1 = g_2 = 5$ and $g_3 = g_4 = 4$) with the case when an unweighted cluster state is used, i.e., a cluster state with unit weight coefficients ($g_1 = g_2 = g_3 = g_4 = 1$). It is this state that is often considered by researchers as a universal state for implementing quantum Gaussian transformations [41,51]. Computation errors when using these two cluster states are shown in Fig. 4. We can see that errors of computation on the weighted cluster state with optimized weight coefficients are always lower than on the unweighted cluster state. In other words, we have found that a weighted cluster state with optimized weight coefficients is better suited for the computation.

After we make the optimization of errors due to the weight coefficients, we can proceed to optimization due to the phase θ_4' of the homodyne detector. Until now, we have considered only the simplest case, when $\theta_4' = \pi/2$. As follows from Eq. (26), this case is optimal if the weight coefficients obey the conditions $g_1 \gg g_4$, $g_2 \gg g_3$, $g_3 \gg 1$, and $g_4 \gg 1$. As we find out, in reality, the weight coefficients are very limited in value. This limitation means that we cannot achieve the minimum error limit (26). This means that the value of the phase $\theta_4' = \pi/2$ is not necessarily optimal. It follows from Eq. (25) that by selecting the phase θ_4' for each specific transformation (for specific b and d), we can minimize the errors. It is this optimization that we carry out below.

The optimization process consists in finding the minimum value of the function $\|\langle\delta\hat{\mathbf{e}}_0^2\rangle\|_\infty = h(\theta_4', b, d)$ by the parameter θ_4' depending on b and d. As a result of the optimization, we obtain the dependence of the optimal phase on the operation, i.e., $\theta_{4,\min}' = f(b, d)$. Figure 5(a) shows the error surfaces of computations on the cluster state with weight coefficients $g_1 = g_2 = 5$ and $g_3 = g_4 = 4$ when the phase $\theta_4' = \pi/2$ and when the phase is optimized depending on the operation [$\theta_4' = \theta_{4,\min}' = f(b, d)$]. It can be seen from the figure that the errors of single-mode transformation at the optimized phase θ_4' are always smaller than the errors at $\theta_4' = \pi/2$. In other words, the error of any single-mode operation can be further decreased by optimizing the phase of the homodyne detector.

To demonstrate the superiority of our optimized scheme (with optimized weight coefficients and optimized phase θ_4'), let us compare it with the case of computations on a cluster state with the maximum weight coefficients ($g_1 = g_2 = g_3 = g_4 = 5$) at $\theta_4' = \pi/2$. Figure 5(b) shows the errors $\|\langle\delta\hat{\mathbf{e}}_0^2\rangle\|_\infty$ obtained by transformations in these two schemes. It can be seen from the graph that the error in the optimized case of computations is less than the error obtained when using the cluster with maximum weight coefficients. It is important to note that to create a cluster with large weight coefficients, we need to implement a squeezing transformation with a large coefficient s [see Eq. (29)]. To perform such a transformation, we need an additional resource. Without loss of generality, we can say that additional energy is required. The larger the squeezing coefficient s, the more energy needed. All this means that it takes more energy to create a cluster with maximum weight coefficients than to create an optimized cluster state. Thus, we can conclude that the smart use of the available physical resource (proper distribution of weight coefficients and smart choice of phases of the homodyne measurement) helps to reduce the quantum computation error.

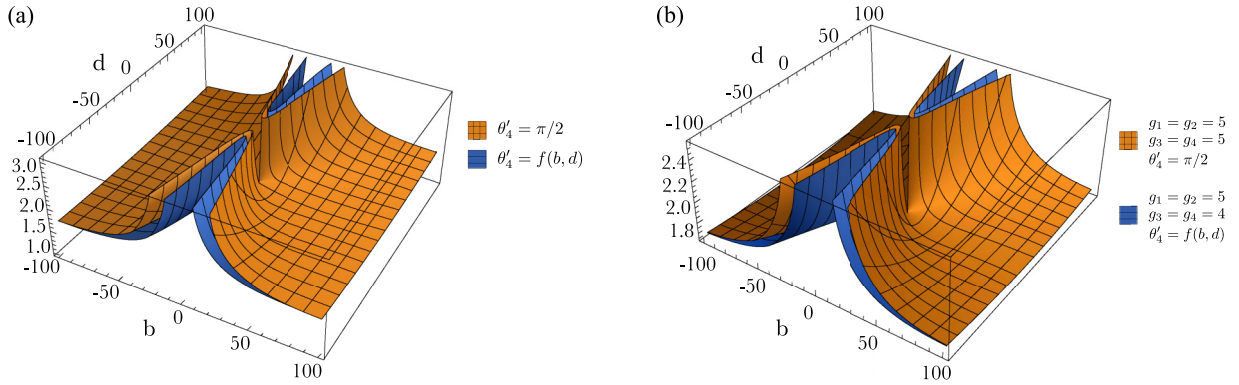

FIG. 5. Distribution of single-mode transformation errors $\|\langle\delta\hat{\mathbf{e}}_0^2\rangle\|_\infty/\langle\delta\hat{y}_s^2\rangle$ depending on b and d [see Eq. (15)]. (a) Transformations performed on the cluster state with optimized weight coefficients. In the diagram, the upper surface corresponds to the case when the phase of the homodyne detector is kept constant $\theta_4' = \pi/2$. The lower surface corresponds to the case when the phase is optimized for the performed transformation (for b and d). (b) In the diagram, the upper surface corresponds to computations on the cluster state with weight coefficients $g_1 = g_2 = g_3 = g_4 = 5$ and the phase $\theta_4' = \pi/2$. The lower surface corresponds to computations on the cluster state with optimized weight coefficients $g_1 = g_2 = 5$ and $g_3 = g_4 = 4$ and optimized homodyne detector phase $\theta_4' = f(b,d)$.

III. SINGLE-MODE OPERATION USING A CUBIC PHASE GATE

A. Transformation scheme with a cubic phase gate

As we have shown in the preceding section, the single-mode Gaussian transformation on a linear four-node weighted cluster state is arbitrary. Also, it is possible to reduce the error of this transformation by optimizing the weight coefficients of the cluster state. However, part of the operations still has significant errors.

In Ref. [36] we showed that it is possible to reduce the teleportation error by using the cubic phase gate to prepare a non-Gaussian resource state. In this section we apply this technique to decrease the error of the arbitrary single-mode Gaussian transformation scheme on a four-node cluster state. To do it, we include the non-Gaussian state as the second node of the cluster [Fig. 6(a)]. It can be seen from Eq. (24) that the expression for the x-quadrature error has a term depending on the phase θ_4. We cannot suppress this term by the CZ gate weight coefficients. It arises as a consequence of the finite squeezing of the second resource oscillator, which is why we replace the second node with a non-Gaussian resource.

As in the previous scheme, we use oscillators squeezed in the y quadrature as a resource for cluster state preparation. A non-Gaussian resource is prepared by sequentially applying the phase shift on $\pi/2$,

$$\hat{R}_2(\pi/2) = e^{i(\pi/2)\hat{a}_2^\dagger\hat{a}_2}, \tag{34}$$

y-quadrature displacement on $\alpha > 0$,

$$\hat{Y}_2(\alpha) = e^{2i\alpha\hat{x}_2}, \tag{35}$$

and a cubic phase gate

$$\hat{Q}_2(\gamma) = e^{-2i\gamma\hat{y}_2^3}, \tag{36}$$

where γ is the coefficient of nonlinearity [see Fig. 6(b)]. Thus, the second recourse oscillator will proceed to the non-Gaussian state, which is described by the following equation:

$$\hat{a}_2 = -\hat{y}_{s,2} + 3\gamma(\alpha + \hat{x}_{s,2})^2 + i(\alpha + \hat{x}_{s,2}). \tag{37}$$

The cubic phase gate (36) deforms the uncertainty region of the squeezed in the x-quadrature state in such a way that a parabola is formed on the phase plane. However, when we displace the y quadrature by a positive value α that satisfies the condition $\alpha^2 \gg \langle\hat{x}_{s,2}^2\rangle$, the quadrature values of the second oscillator will lie in the first quadrant of the phase plane. In other words, only one of the branches of the parabola will remain on the phase plane.

As in the preceding section, let us start with the analysis of the transformation performed on the first pair of resource states. The first Gaussian and second non-Gaussian resource oscillators are entangled using the CZ transformation with the weight coefficient g_1 and the input state is entangled with the first resource oscillator by the CZ gate with a weight coefficient g_4. After the entanglement, the amplitudes of the oscillators are described by the following equations:

$$\hat{a}_{\text{in}}' = \hat{x}_{\text{in}} + i(\hat{y}_{\text{in}} + g_4\hat{x}_{s,1}), \tag{38}$$

$$\hat{a}_1' = \hat{x}_{s,1} + i[\hat{y}_{s,1} - g_1\hat{y}_{s,2} + 3g_1\gamma(\alpha + \hat{x}_{s,2})^2 + g_4\hat{x}_{\text{in}}], \tag{39}$$

$$\hat{a}_2' = -\hat{y}_{s,2} + 3\gamma(\alpha + \hat{x}_{s,2})^2 + i(\alpha + \hat{x}_{s,2} + g_1\hat{x}_{s,1}). \tag{40}$$

We can see that the first resource oscillator is now containing the nonlinearity from the non-Gaussian oscillator due to entanglement. We then perform homodyne measurements with the local oscillator's phases θ_1 and θ_2 over the input and first resource oscillators, respectively. Thus, for the operators of the photocurrent we get

$$\hat{i}_{\text{in}} = \beta\sin\theta_1(\hat{y}_{\text{in}} + g_4\hat{x}_{s,1}) + \beta\cos\theta_1\hat{x}_{\text{in}}, \tag{41}$$

$$\hat{i}_1 = \beta\cos\theta_2\hat{x}_{s,1} + \beta\sin\theta_2[\hat{y}_{s,1} - g_1\hat{y}_{s,2} + 3g_1\gamma(\alpha + \hat{x}_{s,2})^2 + g_4\hat{x}_{\text{in}}], \tag{42}$$

where β is the amplitude of the homodyne detector's local oscillator. Due to the entanglement of the resource state, such a measurement leads to a change in the quadrature components

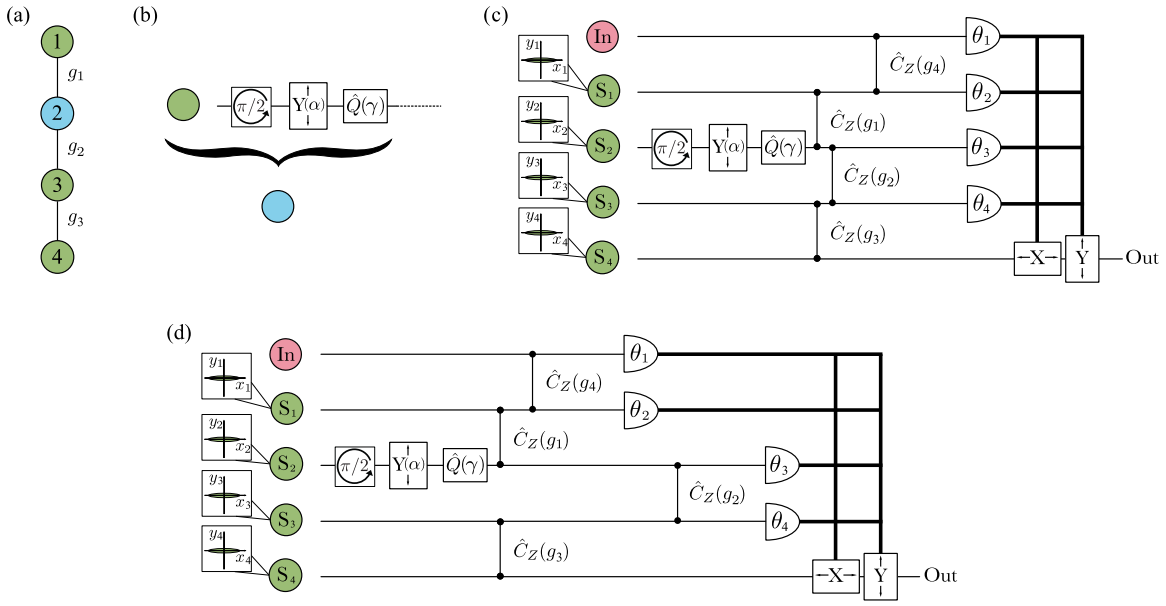

FIG. 6. (a) Configuration of the cluster state used as a resource for computation: Gaussian nodes are shown in green and non-Gaussian nodes are shown in blue. (b) Scheme of non-Gaussian resource state preparation. (c) Scheme for implementing the arbitrary single-mode Gaussian operation on a linear weighted four-node cluster state using a cubic phase gate. (d) Scheme of implementation of arbitrary single-mode Gaussian operation on a pair of two-node cluster states using a cubic phase gate. In the diagram $Y(\alpha)$ is the operation that displaces y quadrature on a real value α and $\hat{Q}(\gamma)$ is the cubic phase gate with nonlinearity γ.

of the field in the second channel:

$$\hat{x}_2' = \left(\frac{\cot\theta_1\cot\theta_2}{g_1g_4} - \frac{g_4}{g_1}\right)\hat{x}_{\rm in} + \frac{\cot\theta_2}{g_1g_4}\hat{y}_{\rm in} - \frac{\hat{y}_{s,1}}{g_1} + \frac{i_{1,m}}{\beta g_1\sin\theta_2} - \frac{i_{{\rm in},m}\cot\theta_2}{\beta g_1g_4\sin\theta_1}, \tag{43}$$

$$\hat{y}_2' = -\frac{g_1\cot\theta_1}{g_4}\hat{x}_{\rm in} - \frac{g_1}{g_4}\hat{y}_{\rm in} + \frac{i_{{\rm in},m}g_1}{\beta g_4\sin\theta_1} + \frac{1}{\sqrt{3\gamma}}\sqrt{\frac{i_{1,m}}{\beta g_1\sin\theta_2} - \frac{i_{{\rm in},m}\cot\theta_2}{\beta g_1g_4\sin\theta_1} + \left(\frac{\cot\theta_1\cot\theta_2}{g_1g_4} - \frac{g_4}{g_1}\right)\hat{x}_{\rm in} + \frac{\cot\theta_2}{g_1g_4}\hat{y}_{\rm in} - \frac{\hat{y}_{s,1}}{g_1} + \hat{y}_{s,2}}. \tag{44}$$

Here, as in the preceding section, we replaced the operators of photocurrents with c-numbers corresponding to the results of the given measurement: $i_{1,m}$ and $i_{{\rm in},m}$. In contrast to Eqs. (8) and (9) for a Gaussian cluster, due to a non-Gaussian resource, a square root in Eq. (44) for the y quadrature arises that determines the transformation error. Note that, as for the teleportation [36], due to the large displacement $\alpha > 0$, it is necessary to take into account only positive values of the square root. To simplify further equations, we introduce new notation

$$I_m = \frac{i_{1,m}}{\beta g_1\sin\theta_2} - \frac{i_{{\rm in},m}\cot\theta_2}{\beta g_1g_4\sin\theta_1}. \tag{45}$$

We can decompose the square root in Eq. (44) in a series in terms of

$$\frac{1}{I_m}\left[\left(\frac{\cot\theta_1\cot\theta_2}{g_1g_4} - \frac{g_4}{g_1}\right)\hat{x}_{\rm in} + \frac{\cot\theta_2}{g_1g_4}\hat{y}_{\rm in} - \frac{\hat{y}_{s,1}}{g_1} + \hat{y}_{s,2}\right],$$

keeping only the first term in the expansion

$$\hat{y}_2' = -\frac{g_1\cot\theta_1}{g_4}\hat{x}_{\rm in} - \frac{g_1}{g_4}\hat{y}_{\rm in} + \frac{i_{{\rm in},m}g_1}{\beta g_4\sin\theta_1} + \sqrt{\frac{I_m}{3\gamma}}$$

$$+ \frac{1}{\sqrt{12\gamma I_m}}\left[\left(\frac{\cot\theta_1\cot\theta_2}{g_1g_4} - \frac{g_4}{g_1}\right)\hat{x}_{\rm in} + \frac{\cot\theta_2}{g_1g_4}\hat{y}_{\rm in} - \frac{\hat{y}_{s,1}}{g_1} + \hat{y}_{s,2}\right]. \tag{46}$$

The termination of the series is correct under the assumption that all moments of the expansion parameter are small. For Gaussian input states, it suffices to satisfy the inequalities

$$3\gamma\alpha^2 \gg \left(\frac{\cot\theta_1\cot\theta_2}{g_1g_4} - \frac{g_4}{g_1}\right)\langle\hat{x}_{\rm in}\rangle + \left(\frac{\cot\theta_2}{g_1g_4}\right)\langle\hat{y}_{\rm in}\rangle, \tag{47}$$

$$(3\gamma\alpha^2)^2 \gg \left(\frac{\cot\theta_1\cot\theta_2}{g_1g_4} - \frac{g_4}{g_1}\right)^2\langle\hat{x}_{\rm in}^2\rangle + 2\left(\frac{\cot\theta_1\cot\theta_2}{g_1g_4} - \frac{g_4}{g_1}\right)\left(\frac{\cot\theta_2}{g_1g_4}\right)\langle\hat{x}_{\rm in}\rangle\langle\hat{y}_{\rm in}\rangle + \left(\frac{\cot\theta_2}{g_1g_4}\right)^2\langle\hat{y}_{\rm in}^2\rangle + \frac{\langle\hat{y}_{s,1}^2\rangle}{g_1^2} + \langle\hat{y}_{s,2}^2\rangle. \tag{48}$$

Note that this requirement limits the protocol's applicability. Below we will discuss in detail how significant this limitation is.

Thus, after measurements over the oscillators in the input and first channels, the quadratures of the second oscillator take the form

$$\begin{pmatrix}\hat{x}_2'\\ \hat{y}_2'\end{pmatrix}=\begin{pmatrix}1 & 0\\ \frac{1}{\sqrt{12\gamma I_m}} & 1\end{pmatrix}\left[\begin{pmatrix}\frac{\cot\theta_1\cot\theta_2}{g_1g_4}-\frac{g_4}{g_1} & \frac{\cot\theta_2}{g_1g_4}\\ -\frac{g_1\cot\theta_1}{g_4} & -\frac{g_1}{g_4}\end{pmatrix}\begin{pmatrix}\hat{x}_{\rm in}\\ \hat{y}_{\rm in}\end{pmatrix}+\begin{pmatrix}-\frac{\hat{y}_{s,1}}{g_1}\\ \frac{\hat{y}_{s,2}}{\sqrt{12\gamma I_m}}\end{pmatrix}\right]+\begin{pmatrix}I_m\\ \frac{i_{{\rm in},m}}{\beta g_2\sin\theta_1}+\sqrt{\frac{I_m}{3\gamma}}\end{pmatrix}. \tag{49}$$

Let us compare the resulting expression with Eq. (10) for the transformation on a pair of Gaussian resource oscillators. One can see that the nonlinearity of the cubic phase gate leads to the appearance of an additional deformation [the matrix before the square brackets on the right-hand side of Eq. (49)]. At the same time, the deformation coefficient depends on the measured values of the photocurrents, which is why we cannot control it. Therefore, we need to compensate for this deformation. Otherwise, it will distort the result and we can significantly increase the error.

The operation on the second pair of nodes does not contain nonlinearity, so it is similar to the transformation (10) up to weight coefficients. At the output of the scheme, the c-number components of the quadratures of the field are compensated by displacement, depending on the values of the measured photocurrents. In addition, we explore the notation in (11), as in the preceding section. Then the transformation performed on the input oscillator has the form

$$\begin{pmatrix}\hat{x}_{\rm out}\\ \hat{y}_{\rm out}\end{pmatrix}=\begin{pmatrix}\frac{\cot\theta_3\cot\theta_4'-1}{g_3/g_2} & \frac{\cot\theta_4'}{g_3/g_2}\\ -\frac{g_3\cot\theta_3}{g_2} & -\frac{g_3}{g_2}\end{pmatrix}\begin{pmatrix}1 & 0\\ \frac{1}{\sqrt{12\gamma I_m}} & 1\end{pmatrix}\times\left[\begin{pmatrix}\frac{\cot\theta_1\cot\theta_2'-1}{g_1/g_4} & \frac{\cot\theta_2'}{g_1/g_4}\\ -\frac{g_1\cot\theta_1}{g_4} & -\frac{g_1}{g_4}\end{pmatrix}\begin{pmatrix}\hat{x}_{\rm in}\\ \hat{y}_{\rm in}\end{pmatrix}+\begin{pmatrix}-\frac{\hat{y}_{s,1}}{g_1}\\ \frac{\hat{y}_{s,2}}{\sqrt{12\gamma I_m}}\end{pmatrix}\right]+\begin{pmatrix}-\frac{\hat{y}_{s,3}}{g_3}\\ \hat{y}_{s,4}\end{pmatrix}. \tag{50}$$

Now let us find if it is possible to compensate for the deformation that occurs due to the presence of the cubic phase state. This deformation leads to a distortion of the oscillator basis at the output of the first part of the scheme. Therefore, knowing the measurement results in the first part of the scheme, we have the opportunity to remove this deformation by correcting the measurement basis in the second part of the scheme. To do so, we rewrite Eq. (50), including the deformation in the matrix of the second part of the protocol:

$$\begin{pmatrix}\hat{x}_{\rm out}\\ \hat{y}_{\rm out}\end{pmatrix}=\begin{pmatrix}\frac{g_2}{g_3}\left[\left(\cot\theta_3+\frac{1}{\sqrt{12\gamma I_m}}\right)\cot\theta_4-1\right] & \frac{g_2}{g_3}\cot\theta_4\\ -\frac{g_3}{g_2}\left(\cot\theta_3+\frac{1}{\sqrt{12\gamma I_m}}\right) & -\frac{g_3}{g_2}\end{pmatrix}\times\left[\begin{pmatrix}\frac{\cot\theta_1\cot\theta_2-1}{g_1/g_4} & \frac{\cot\theta_2}{g_1/g_4}\\ -\frac{g_1\cot\theta_1}{g_4} & -\frac{g_1}{g_4}\end{pmatrix}\begin{pmatrix}\hat{x}_{\rm in}\\ \hat{y}_{\rm in}\end{pmatrix}+\begin{pmatrix}-\frac{\hat{y}_{s,1}}{g_1}\\ \frac{\hat{y}_{s,2}}{\sqrt{12\gamma I_m}}\end{pmatrix}\right]+\begin{pmatrix}-\frac{\hat{y}_{s,3}}{g_3}\\ \hat{y}_{s,4}\end{pmatrix}. \tag{51}$$

If we introduce the new phase

$$\cot\theta_3'=\cot\theta_3+\frac{1}{\sqrt{12\gamma I_m}}, \tag{52}$$

then the transformation over the input oscillator will be determined by the matrix (13) depending on θ_3'. In other words, according to the measurements results on the input and the first resource oscillators, we can adjust the phase θ_3 to compensate for the additional deformation. Thus, we can perform the given operation without additional distortion. As a result, in the modified scheme, the transformation performed on the input state is the same as the transformation to Eq. (12), but it has a different error:

$$\begin{pmatrix}\hat{x}_{\rm out}\\ \hat{y}_{\rm out}\end{pmatrix}=U(\theta_1,\theta_2',\theta_3',\theta_4')\begin{pmatrix}\hat{x}_{\rm in}\\ \hat{y}_{\rm in}\end{pmatrix}+\delta\hat{\mathbf{e}}(\theta_3',\theta_4'). \tag{53}$$

Here the matrix U is defined by Eq. (13) and the error is given by

$$\delta\hat{\mathbf{e}}_0(\theta_3',\theta_4')=\begin{pmatrix}\frac{\cot\theta_3'\cot\theta_4'-1}{g_3/g_2} & \frac{\cot\theta_4'}{g_3/g_2}\\ -\frac{g_3\cot\theta_3'}{g_2} & -\frac{g_3}{g_2}\end{pmatrix}\begin{pmatrix}-\frac{\hat{y}_{s,1}}{g_1}\\ \frac{\hat{y}_{s,2}}{\sqrt{12\gamma I_m}}\end{pmatrix}+\begin{pmatrix}-\frac{\hat{y}_{s,3}}{g_3}\\ \hat{y}_{s,4}\end{pmatrix}. \tag{54}$$

Thus, the conversion error depends not only on the phases θ_3' and θ_4', but also on the measured value I_m.

We have found that the considered scheme with a cubic phase gate implements the same transformation as the scheme with a Gaussian cluster considered in the preceding section. Thus, we do not need to justify the arbitrariness of this transformation. However, the errors of these two operations differ significantly from each other. Next we compare the computation errors of the two schemes and evaluate the limitations of the scheme with a cubic phase gate.

B. Error of transformation with the cubic phase gate

Let us now investigate how the error of computation in the modified scheme has changed. As in the preceding section, we assume the Gaussian resource states to be squeezed equally ($\langle\hat{y}_{s,j}^2\rangle\equiv\langle\delta\hat{y}_s^2\rangle$ for $j\in 1,2,3,4$). Then the variances of the error vector are

$$\langle\delta\hat{\mathbf{e}}_0^2\rangle=\begin{pmatrix}\frac{1}{g_1^2}\left(\frac{\cot\theta_3'\cot\theta_4'-1}{g_3/g_2}\right)^2+\frac{1}{12\gamma I_m}\left(\frac{\cot\theta_4'}{g_3/g_2}\right)^2+\frac{1}{g_3^2}\\ \frac{1}{g_1^2}\left(\frac{g_3\cot\theta_3'}{g_2}\right)^2+\frac{1}{12\gamma I_m}\frac{g_3^2}{g_2^2}+1\end{pmatrix}\times\left\langle\delta\hat{y}_s^2\right\rangle. \tag{55}$$

Comparing Eqs. (24) and (55), we can see that the second term in the expressions for quadrature errors is smaller in $12\gamma I_m$. The average value of I_m is proportional to the displacement α of the resource state quadrature; therefore, with a sufficient displacement α, we can significantly decrease the contribution to the error from these terms.

As in the preceding section, we consider the norm $\|\cdot\|_\infty$ as a measure of errors. We estimate the value of I_m as its average value, i.e., $\langle I_m\rangle\approx 3\gamma\alpha^2$. We use a relatively small cubic phase gate coefficient $\gamma=0.1$ [42,46] and the

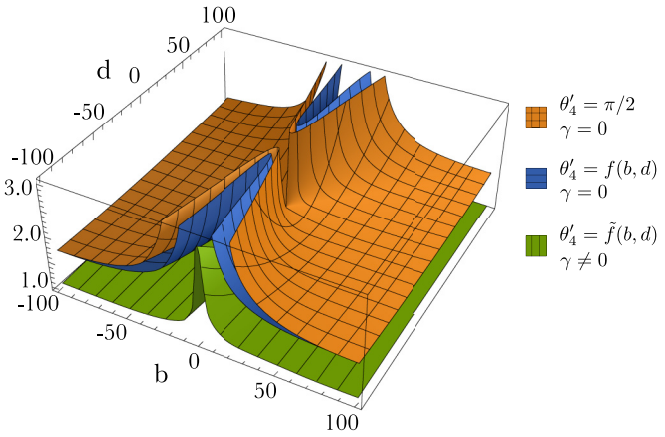

FIG. 7. Distribution of single-mode transformation errors $\|\langle\delta\hat{\mathbf{e}}_0^2\rangle\|_\infty/\langle\delta\hat{y}_s^2\rangle$. The graph demonstrates three error distributions depending on the implemented operation, i.e., depending on b and d [see Eq. (15)]. All three distributions are calculated for optimized weight coefficients ($g_1 = g_2 = 5$ and $g_3 = g_4 = 4$). The orange (upper) and blue (middle) surfaces correspond to errors for the scheme without a cubic phase gate ($\gamma = 0$): The orange (upper) surface corresponds to the case of a fixed phase value $\theta_4' = \pi/2$ and the blue (middle) surface corresponds to the case when the angle θ_4' optimization is performed ($\theta_4' = \tilde{f}(b,d)$). The green (lower) surface corresponds to the error of the scheme using the cubic phase gate ($\gamma \neq 0$) with θ_4' being optimized.

displacement $\alpha = 5\sqrt{5}$ (i.e., $12\gamma I_m = 45$) in the calculations. This displacement satisfies the condition $\alpha^2 \gg \langle\hat{x}_{s,2}^2\rangle$ required for the correct operation of the protocol and is implemented in practice. Figure 7 demonstrates a comparison of error surfaces for a scheme without and with a cubic phase gate. One can see that the error of the scheme with a cubic phase gate turns out to be smaller for the entire range of transformations. In addition, it suppresses the increase of the error in the vicinity of $b = 0$. Thus, the inclusion in the cluster of a non-Gaussian resource obtained using a cubic phase gate further reduces the computation error.

Let us recall that the proposed protocol can operate under the condition of low nonlinearity of the cubic phase gate. We can compensate for a small value of γ by a large value of displacement α. This is an important advantage, since increasing the transformation coefficient γ of the cubic phase gate is a difficult experimental problem.

IV. EVALUATION OF THE OPTIMIZATION EFFICIENCY OF ONE-WAY QUANTUM COMPUTATION

In the previous sections, we have shown that one-way computations on a four-node cluster state can be optimized by choosing weight coefficients as well as the use of non-Gaussian transformations. The optimization leads to a decrease of the computation errors. Now we need to discuss how effective these optimizations are. What is the gain in decreasing errors if we apply all the proposed optimizations?

To answer these questions, we first need to understand how the resulting errors can be compared with each other and what advantages we can expect from the proposed optimization. To do this, we recall the quantum error correction procedure. In one-way quantum computations, the error displaces the quadrature of the state under computation by a small value proportional to the squeezed quadrature variance of the resource oscillator. In [37] the authors proposed a method for correcting errors of small quadrature displacements using the so-called Gottesman-Kitaev-Preskill (GKP) states. In [23] this method was applied theoretically to the problem of error correction of one-way computation. In [52] we refined the error correction method for one-way computations taking into account the noise inherent in the error correction procedure itself, i.e., nonideal GKP states. Omitting all the theoretical details, we can conclude the probability that the error has not been corrected is [52]

$$P_{\text{err}}(x_{\text{err}}, y_{\text{err}}) = 1 - \text{erf}\left(\frac{\sqrt{\pi}}{2\sqrt{2}\sqrt{\langle\delta\hat{y}_s^2\rangle\left(x_{\text{err}} + \frac{\sqrt{5}+1}{2}\right)}}\right) \times \text{erf}\left(\frac{\sqrt{\pi}}{2\sqrt{2}\sqrt{\langle\delta\hat{y}_s^2\rangle(y_{\text{err}} + \sqrt{5} + 1)}}\right), \quad (56)$$

where $x_{\text{err}}\langle\delta\hat{y}_s^2\rangle$ is the error variance of the x quadrature of the output target oscillator and $y_{\text{err}}\langle\delta\hat{y}_s^2\rangle$ is the error variance of the y quadrature. The arguments of the functions erf are determined by two factors: The variances of the transformation errors of each quadrature (the first terms in the denominators of the arguments) and the error added when performing error correction. The latter factor is also the sum of two contributions: The error from the performing of operation sum(1) and the error from the broadening of the GKP state peaks. Note that the order of the correction procedure determines the distinction of x- and y-quadrature errors. The error function $\text{erf}(1/z)$ is monotonically decreasing, so the greater the value is of error variance of quadratures, the more likely the errors have not been corrected.

As can be seen from the definition of the function $P_{\text{err}}(x_{\text{err}}, y_{\text{err}})$, it reveals the quality of computation and characterizes its scale. Accordingly, it is convenient to utilize this function as a measure for comparing optimized and nonoptimized computations and for evaluating the efficiency of the optimization procedure. Figure 8 demonstrates the ratios of the error probabilities $P_{\text{err}}(x_{\text{err}}, y_{\text{err}})/P_{\text{err}}(x_{\text{err}}^{\text{opt}}, y_{\text{err}}^{\text{opt}})$, where $P_{\text{err}}(x_{\text{err}}, y_{\text{err}})$ is the error probability of nonoptimized computation and $P_{\text{err}}(x_{\text{err}}^{\text{opt}}, y_{\text{err}}^{\text{opt}})$ is the error probability of optimized computation. Nonoptimized computations correspond to ones on the unweighted cluster state with $\theta_4' = \pi/2$. Optimized computations correspond to the ones discussed in Fig. 7: (i) optimization by weight coefficients ($g_4 = g_3 = 4$ and $g_2 = g_1 = 5$) and $\theta_4' = \pi/2$, (ii) optimization by weight coefficients and by the phase of the homodyne measurement [$\theta_4' = f(b,d)$], and (iii) optimization by weight coefficients, by the phase of homodyne detector, and using a cubic phase gate. All graphs are calculated for squeezing of -15 dB. When we perform the optimization only by weight coefficients, the error probability for some transformations becomes 45 times lower. If in addition we perform optimization via the phases of the homodyne detector, the gain for some operations is 400

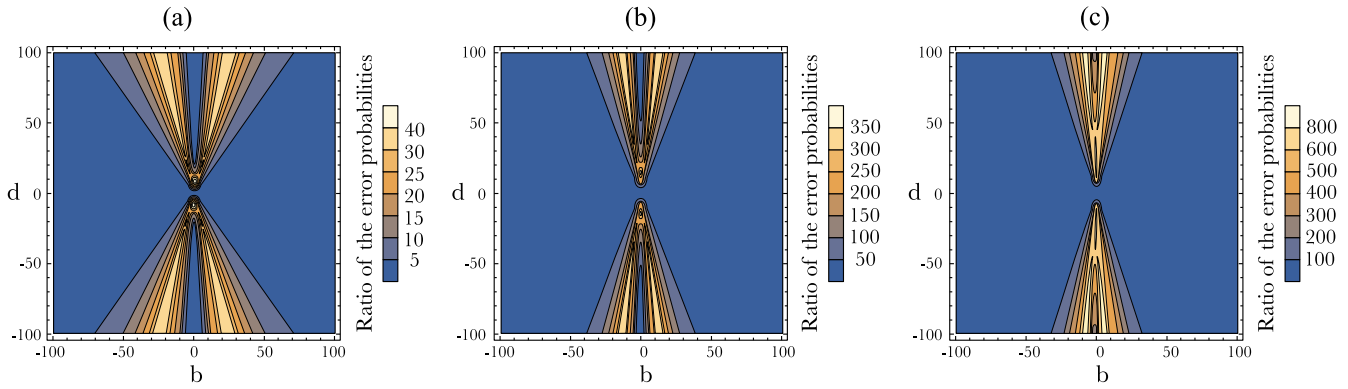

FIG. 8. Ratios of the error probabilities $P_{\rm err}(x_{\rm err}, y_{\rm err})/P_{\rm err}(x_{\rm err}^{\rm opt}, y_{\rm err}^{\rm opt})$, depending on b and d [see Eq. (15)]. Here $P_{\rm err}(x_{\rm err}, y_{\rm err})$ is the error probability of nonoptimized computations and $P_{\rm err}(x_{\rm err}^{\rm opt}, y_{\rm err}^{\rm opt})$ is the error probability of optimize computations. In the diagram, (a) optimization is performed by weight coefficients ($g_4 = g_3 = 4$, $g_2 = g_1 = 5$, and $\theta_4' = \pi/2$), (b) optimization is performed by weight coefficients and the phase of the homodyne detector, and (c) full optimization is performed and the cubic phase gate is used.

times higher. When we use a cubic phase gate and perform full optimization, the error probability for some transformations is 900 times smaller. Note that for resource oscillators with less squeezing, the benefit from the optimization procedure is even more significant.

Thus, the proposed optimization works very effectively. We can decrease the error probability in the results of computations after the correction procedure by several orders of magnitude. This means that the optimized computation scheme is more fault tolerant. The fault-tolerant universal quantum computation in the proposed scheme requires less squeezing than has been suggested earlier [23].

V. CONCLUSION

In the work presented, we have shown that by varying the weight coefficients of the cluster state, which were used as a resource for computations, we could decrease the error of arbitrary single-mode Gaussian transformations. In real experiments, the squeezing resource is not infinite. Its proper distribution in the cluster is required. We estimated the upper value of the weight coefficients that could be obtained with the current experimental capabilities. We have shown that the ratios of weight coefficients play a significant role in decreasing the error. Proper distribution of weight coefficients allowed us to decrease the error for most of the single-mode Gaussian operations while spending less energy.

For nonuniversal operations, it is possible to select the cluster state configuration that provides minimal computation error. Generally, the problem of multidimensional optimization is extremely complex. Its complexity is determined both by the dimension of the cluster and by the infinite dimensions of the transformation space. Nevertheless, it is possible to select a weight coefficient which provides a minimal error for most of the operations.

Another useful tool is optimization by phases of homodyne measurements. Unlike the weight coefficients, we can choose the optimal phases for each specific operation. This strategy allows us to decrease the computation error without using any additional resources.

We have shown that the inclusion of non-Gaussian nodes prepared by cubic phase gates in the resource cluster state can further decrease the transformation error. For the protocol to work properly, we need to make relatively small displacements of the squeezed state before applying the cubic phase gate. These displacements can be easily implemented in practice. It should be noted that the practical implementation of cubic phase gate is still a challenge for experimentalists. However, the generation of the cubic phase states has recently been demonstrated in the microwave frequency range [50]. There is also an active search for suitable systems for the implementation of non-Gaussian gates in optics [42,44–47,49].

We have demonstrated the effectiveness of our optimization methods. We have shown that it is possible to significantly decrease the probability of wrong error correction using the proposed optimization methods. This makes our scheme more fault tolerant. Thus, the methods considered can provide a significant benefit for arbitrary single-mode Gaussian transformations.

It is important to note that the optimization procedure we proposed does not depend on the way the cluster state was generated or on the encoding of the input states. Regardless of the available experimental resources, it is possible to optimize the scheme to minimize the quantum computation error.

We leave for future work the generalization of our proposed optimization method to reduce errors in two-mode Gaussian and non-Gaussian transformations. Since all these transformations are needed to implement a universal quantum computer [1], their optimization will help make quantum computation more tolerant to errors. It will help reduce the requirements on squeezing for the resources used.

ACKNOWLEDGMENTS

Section II was supported by the Theoretical Physics and Mathematics Advancement Foundation BASIS (Grant No. 21-1-4-39-1). Sections III and IV were supported by the Russian Science Foundation (Grant No. 22-22-00022).

[1] S. Lloyd and S. L. Braunstein, Phys. Rev. Lett. **82**, 1784 (1999).
[2] N. C. Menicucci, P. van Loock, M. Gu, C. Weedbrook, T. C. Ralph, and M. A. Nielsen, Phys. Rev. Lett. **97**, 110501 (2006).
[3] R. Raussendorf and H. J. Briegel, Phys. Rev. Lett. **86**, 5188 (2001).
[4] M. A. Nielsen, Rep. Math. Phys. **57**, 147 (2006).
[5] S. Yokoyama, R. Ukai, S. C. Armstrong, C. Sornphiphatphong, T. Kaji, S. Suzuki, J.-i. Yoshikawa, H. Yonezawa, N. C. Menicucci, and A. Furusawa, Nat. Photon. **7**, 982 (2013).
[6] J. Roslund, R. M. de Araújo, S. Jiang, C. Fabre, and N. Treps, Nat. Photon. **8**, 109 (2014).
[7] M. Chen, N. C. Menicucci, and O. Pfister, Phys. Rev. Lett. **112**, 120505 (2014).
[8] J.-i. Yoshikawa, S. Yokoyama, T. Kaji, C. Sornphiphatphong, Y. Shiozawa, K. Makino, and A. Furusawa, APL Photon. **1**, 060801 (2016).
[9] M. V. Larsen, X. Guo, C. R. Breum, J. S. Neergaard-Nielsen, and U. L. Andersen, Science **366**, 369 (2019).
[10] W. Asavanant, Y. Shiozawa, S. Yokoyama, B. Charoensombutamon, H. Emura, R. N. Alexander, S. Takeda, J.-i. Yoshikawa, N. C. Menicucci, H. Yonezawa, and A. Furusawa, Science **366**, 373 (2019).
[11] M. Hein, W. Dür, J. Eisert, R. Raussendorf, M. Van den Nest, and H.-J. Briegel, Quantum computers, algorithms and chaos, in *Proceedings of the International School of Physics "Enrico Fermi," Course CLXII, Varenna, 2005*, edited by G. Casati, D. L. Shepelyansky, P. Zoller, and G. Benenti (IOS, Amsterdam, 2006).
[12] O. Houhou, H. Aissaoui, and A. Ferraro, Phys. Rev. A **92**, 063843 (2015).
[13] L.-h. Sun, Y.-Q. Chen, and G.-x. Li, Opt. Express **20**, 3176 (2012).
[14] C. Gabriel, I. Rigas, A. Aiello, S. Berg-Johansen, P. van Loock, C. Marquardt, and G. Leuchs, Cluster state generation with quadrature squeezed cylindrically polarized modes, in *Conference on Lasers and Electro-Optics 2012, OSA Technical Digest (online)* (Optica Publishing Group, 2012), paper JW4A.102, https://doi.org/10.1364/CLEO_AT.2012.JW4A.102.
[15] K. S. Tikhonov, A. D. Manukhova, S. B. Korolev, T. Yu. Golubeva, and Y. M. Golubev, Opt. Spectrosc. **127**, 878 (2019).
[16] D. F. Milne and N. V. Korolkova, Phys. Rev. A **85**, 032310 (2012).
[17] N. C. Menicucci, S. T. Flammia, H. Zaidi, and O. Pfister, Phys. Rev. A **76**, 010302 (2007).
[18] M. Yukawa, R. Ukai, P. van Loock, and A. Furusawa, Phys. Rev. A **78**, 012301 (2008).
[19] J. Zhang and S. L. Braunstein, Phys. Rev. A **73**, 032318 (2006).
[20] G. Ferrini, J. P. Gazeau, T. Coudreau, C. Fabre, and N. Treps, New J. Phys. **15**, 093015 (2013).
[21] R. Medeiros de Araújo, J. Roslund, Y. Cai, G. Ferrini, C. Fabre, and N. Treps, Phys. Rev. A **89**, 053828 (2014).
[22] H. Vahlbruch, M. Mehmet, K. Danzmann, and R. Schnabel, Phys. Rev. Lett. **117**, 110801 (2016).
[23] N. C. Menicucci, Phys. Rev. Lett. **112**, 120504 (2014).
[24] K. Fukui, A. Tomita, A. Okamoto and K. Fujii, Phys. Rev. X **8**, 021054 (2018).
[25] K. Noh and C. Chamberland, Phys. Rev. A **101**, 012316 (2020).
[26] K. Fukui, arXiv:1906.09767.
[27] K. Noh, C. Chamberland, and F. G. S. L. Brandão, PRX Quantum **3**, 010315 (2022).
[28] M. V. Larsen, C. Chamberland, K. Noh, J. S. Neergaard-Nielsen, and U. L. Andersen, PRX Quantum **2**, 030325 (2021).
[29] J. E. Bourassa, R. N. Alexander, M. Vasmer, A. Patil, I. Tzitrin, T. Matsuura, D. Su, B. Q. Baragiola, S. Guha, G. Dauphinais, K. K. Sabapathy, N. C. Menicucci and I. Dhand, Quantum **5**, 392 (2021).
[30] I. Tzitrin, T. Matsuura, R. N. Alexander, G. Dauphinais, J. E. Bourassa, K. K. Sabapathy, N. C. Menicucci and I. Dhand, PRX Quantum **2**, 040353 (2021).
[31] E. R. Zinatullin, S. B. Korolev, and T. Y. Golubeva, Phys. Rev. A **103**, 062407 (2021).
[32] M. V. Larsen, J. S. Neergaard-Nielsen, and U. L. Andersen, Phys. Rev. A **102**, 042608 (2020).
[33] D. Su, C. Weedbrook, and K. Brádler, Phys. Rev. A **98**, 042304 (2018).
[34] R. N. Alexander, S. C. Armstrong, R. Ukai, and N. C. Menicucci, Phys. Rev. A **90**, 062324 (2014).
[35] J. Niset, J. Fiurášek, and N. J. Cerf, Phys. Rev. Lett. **102**, 120501 (2009).
[36] E. R. Zinatullin, S. B. Korolev, and T. Y. Golubeva, Phys. Rev. A **104**, 032420 (2021).
[37] D. Gottesman, A. Kitaev, and J. Preskill, Phys. Rev. A **64**, 012310 (2001).
[38] T. Opatrný, G. Kurizki and D.-G. Welsch, Phys. Rev. A **61**, 032302 (2000).
[39] P. T. Cochrane, T. C. Ralph and G. J. Milburn, Phys. Rev. A **65**, 062306 (2002).
[40] S. Ghose and B. C. Sanders, J. Mod. Opt. **54**, 855 (2007).
[41] M. Gu, C. Weedbrook, N. C. Menicucci, T. C. Ralph, and P. van Loock, Phys. Rev. A **79**, 062318 (2009).
[42] M. Yukawa, K. Miyata, H. Yonezawa, P. Marek, R. Filip, and A. Furusawa, Phys. Rev. A **88**, 053816 (2013).
[43] Y. Zheng, O. Hahn, P. Stadler, P. Holmvall, F. Quijandría, A. Ferraro, and G. Ferrini, PRX Quantum **2**, 010327 (2021).
[44] W. Asavanant, K. Takase, K. Fukui, M. Endo, J.-i. Yoshikawa, and A. Furusawa, Phys. Rev. A **103**, 043701 (2021).
[45] K. Marshall, R. Pooser, G. Siopsis, and C. Weedbrook, Phys. Rev. A **91**, 032321 (2015).
[46] K. Miyata, H. Ogawa, P. Marek, R. Filip, H. Yonezawa, J.-i. Yoshikawa, and A. Furusawa, Phys. Rev. A **93**, 022301 (2016).
[47] R. Yanagimoto, T. Onodera, E. Ng, L. G. Wright, P. L. McMahon, and H. Mabuchi, Phys. Rev. Lett. **124**, 240503 (2020).
[48] T. Hillmann, F. Quijandría, G. Johansson, A. Ferraro, S. Gasparinetti, and G. Ferrini, Phys. Rev. Lett. **125**, 160501 (2020).
[49] S. Konno, A. Sakaguchi, W. Asavanant, H. Ogawa, M. Kobayashi, P. Marek, R. Filip, J.-i. Yoshikawa, and A. Furusawa, Phys. Rev. Applied **15**, 024024 (2021).
[50] M. Kudra, M. Kervinen, I. Strandberg, S. Ahmed, M. Scigliuzzo, A. Osman, D. P. Lozano, M. O. Tholén, R. Borgani, D. B. Haviland, G. Ferrini, J. Bylander, A. F. Kockum, F. Quijandría, P. Delsing, and S. Gasparinetti, PRX Quantum **3**, 030301 (2022).
[51] R. Ukai, J.-i. Yoshikawa, N. Iwata, P. van Loock, and A. Furusawa, Phys. Rev. A **81**, 032315 (2010).
[52] S. B. Korolev and T. Y. Golubeva, Phys. Lett. A **441**, 128149 (2022).